be stored in active condition for long time. The development of functional protein microarrays for practical use, therefore, requires relatively easy methods for the functional immobilization and purification of freshly prepared proteins on the microplate. We recently developed a high-throughput method for protein synthesis using the wheat germ cell-free protein synthesis and an automatic protein synthesizer (4–6) and demonstrated that the automatic synthesizer is very useful for the production of freshly prepared proteins.

To create a new type of protein microarray, we developed a novel tag using a DNA-binding protein and a newly designed microplate consisting of agarose and commercially available genomic DNAs (7). The new tag, named here as DBtag, is the Arabidopsis transcription factor HY5 having a basic leucine-zipper domain (8). We found that the HY5 protein had high binding affinity to commercially available salmon sperm and calf DNAs. Here, we used this DNA-binding ability of HY5 to immobilize and purify the fusion protein on the microplate.

2. Materials

2.1. DBtag Protein Production

1. PCR thermocycler MP (Takarabio Inc., Otsu, Japan).
2. ExTaq DNA polymerase (Takarabio Inc.).
3. pEU-DBtag (accession no. AB369281) or Arabidopsis *HY5* gene (GenBANK accession no. NM_121164).
4. cDNA for synthesized protein.
5. Oligonucleotide primers.
6. Exonuclease I (1 U/10 μL reaction mixture, GE Healthcare, Little Chalfont, UK).
7. PCR product purification kit (Gel-M®Extraction, Viogene, Shijr, Taipei).
8. 5× Transcription buffer (TB): 400 mM HEPES-KOH, pH 7.8, 80 mM magnesium acetate, 10 mM spermidine, and 50 mM DTT.
9. Nucleotide tri-phosphates (NTPs) mix: a solution containing 25 mM each of ATP, GTP, CTP, and UTP.
10. SP6 RNA polymerase (80 units/μL, Promega; Madison, WI).
11. RNasin (80 units/μL, Promega; Madison, WI).
12. Microcon (YM-50; Millipore, Bedford, USA).

13. 10 mg/mL creatine kinase (Roche Diagnostics K. K.).
14. 4× Translational substrate buffer (TSB): 120 mM HEPES-KOH, pH 7.8, 400 mM potassium acetate, 10.8 mM magnesium acetate, 1.6 mM spermidine, 16 mM DTT, 1.2 mM amino acid mix, 4.8 mM ATP, 1 mM GTP, and 64 mM creatine phosphate. Or, 4× SUB-AMIX® (CellFree Sciences Co., Ltd., Matsuyama, Japan).
15. 1× TSB: 30 mM HEPES-KOH, pH 7.8, 100 mM potassium acetate, 2.7 mM magnesium acetate, 0.4 mM spermidine, 4 mM DTT, 0.3 mM amino acid mix, 1.2 mM ATP, 0.25 mM GTP, and 16 mM creatine phosphate. Or, 1× SUB-AMIX® (CellFree Sciences Co., Ltd.).
16. Wheat embryo extract (240 OD/mL, described in Chapter 3) or WEPRO®1240 (CellFree Sciences Co., Ltd.).
17. *Escherichia coli* biotin protein ligase (BirA, Genbank Accession no. NP_312927).
18. Biotin (Nakalai Tesque, Inc., Kyoto, Japan).

2.2. Protein Microarray Using Garose/DNA Microplate

1. Agarose (SeaKem Gold, Takarabio, Inc.).
2. Salmon sperm DNA (Sigma-Aldrich Corp, MO).
3. 1× TMD buffer: 20 mM Tris–HCl at pH 7.8, 2 mM $MgCl_2$, and 1 mM DTT.
4. Slide glass (Asahi glass, Japan).
5. Lab-Tek II Chamber slide (one-well, Nalge Nunc International Co., Naperville, IL).
6. Pin-type spotter like MultiSPRinter™ spotter (Toyobo Bio Instruments, Tsuruga, Japan) or comparable product.
7. Wash buffer: 20 mM Tris–HCl at pH 7.8, 200 mM NaCl, 2 mM $MgCl_2$, and 1 mM DTT.
8. Tupperware box.

2.3. Functional Protein Analysis Using the Protein Microarray

1. cDNAs.
2. 1× PBS buffer: 137 mM Nacl, 2.7 mM Kcl, 10 mM Na_2HPO_4, 1.8 mM KH_2PO_4, pH 7.4.
3. Kination solution: 50 mM Tris–HCl at pH 7.8, 100 mM NaCl, 10 mM $MgCl_2$, and 0.1 mM DTT, 10,000 Ci/μl [γ-^{32}P]-ATP, 0.05% DMSO (plus protein kinase inhibitor for inhibitor solution, if need be).
4. Caspase-3 solution: 20 mM Tris–HCl at pH 7.8, 200 mM NaCl, 2 mM $MgCl_2$, 1 mM DTT, and 17.4 ng/μL caspase 3 (human, Sigma-Aldrich Corp)].
5. 10μg/ml Alexa488-streptavidin (STA) (Invitrogen Corp., Carlsbad, CA).

6. Typhoon 9400 imaging system (GE Healthcare, Little Chalfont, UK) or comparable product.

3. Methods

3.1. Construction of DNA Template for DBtagged Protein Production

Arabidopsis *HY5* gene was inserted into pEU vector (4) as pEU-DBtag (Fig. 7.1a). The DBtag fragment (accession no. AB369281) was isolated (Subheading 3.1.1.) and fused on N-terminal of purpose gene by split-PCR (Subheading 3.1.2.). We have optimized a PCR-based linear template DNA generation by designing a set of universal primers for fusions of SP6 promoter and translational enhancer (E02) (9). For production of biotinylated protein, biotin ligation site (amino acid sequence: GLNDIFEAQKIEWHE)

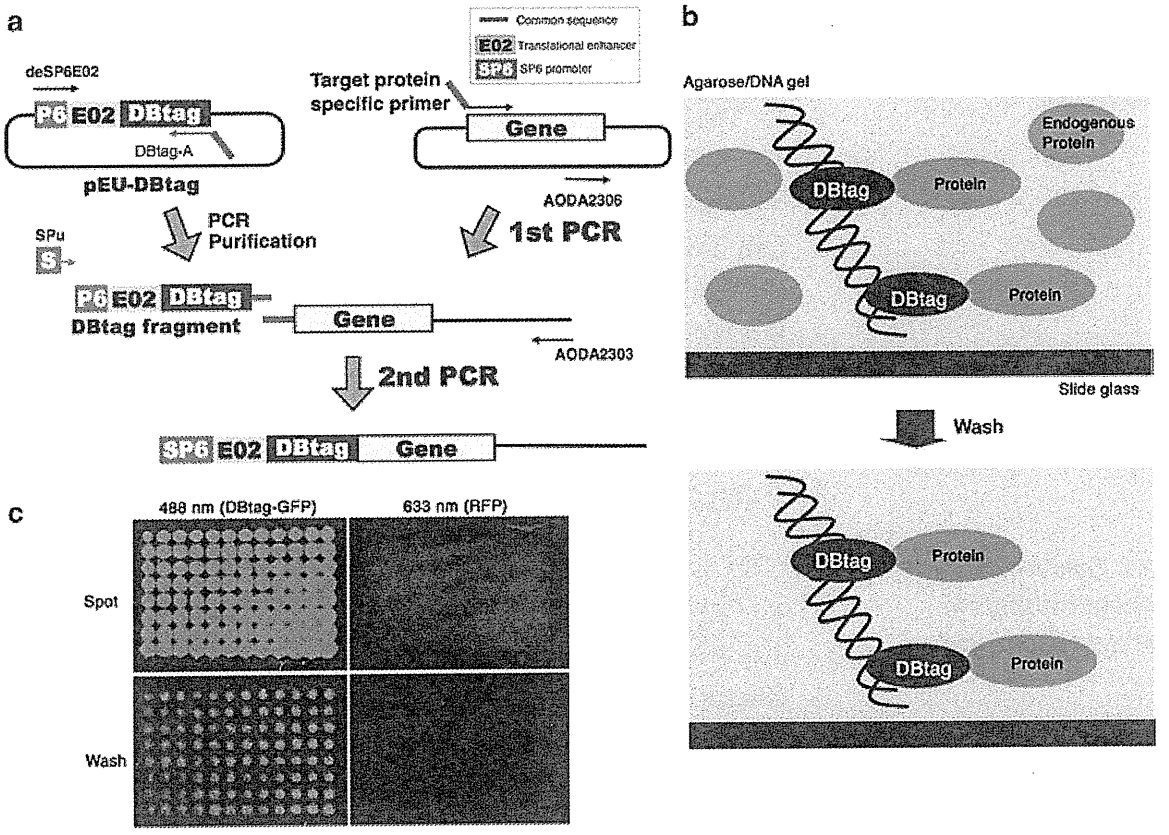

Fig. 7.1. (**a**) Scheme for DBtag-fusion method by the "split-primer" PCR. The DBtag fragment includes partial SP6 promoter. DNA amplification by SPu primer makes full-length SP6 promoter. (**b**) Schematic showing immobilized DBtag-fusion proteins on the microplate before and after washing. (**c**) DBtag-GFP and RFP (untagged) were mixed together and the mixture was spotted on the microplate. The DBtag-GFP was immobilized on the microplate, while the RFP was washed out and no RFP fluorescence was observed. Reproduced from ref. (7) with permission.

is inserted into N- or C-terminal of purpose gene by PCR or general recombinant method.

3.1.1. Isolation of DBtag Fragment

1. Prepare 100 μL of PCR reaction mixture as the manufacturer's instructions (Takarabio Inc.) by mixing 100 pg/μL of plasmid (pEU-DBtag) and 200 nM of deSP6E02 (5′-GGTGACAC TATAGAACTCACCTATCTCTCTACACA) and DBtag-A (5′-TGGTGGTGGTGGGTGGAAGCCCTGGAAG TACAGGTTCTC), 200 μM of each dNTP, 1.25 units of ExTaq DNA polymerase.
2. Set the mixture to PCR thermocycler for 1 min denaturation at 96°C followed by 25 cycles of amplification: 98°C for 10 s, 55°C for 30 s, and 72°C for 1 min.
3. Incubate the amplified product with exonuclease I (1 U/10 μL reaction mixture) for 30 min at 37°C, and then treat for 30 min at 80°C (see Note 1).
4. Purify them with a PCR product purification kit.
5. Check concentration of the DBtag fragment.

3.1.2. Construction of DNA Template for DBtag Protein by Split-PCR

1. Prepare 50 μL of a first PCR reaction mixture by mixing 3 ng of plasmid or 3 μL of *Escherichia coli* (overnight culture) as template, 200 μM each of dNTP, 1.5 units of ExTaq DNA polymerase, 10 nM of target protein-specific primer (5′-CCACCCACCACCACCAatgnnnnnnnnnnnnnnnn; uppercase and lowercase indicate common sequence and the 5′-coding region of the target gene, respectively) and AODA2306 primer (5′-AGCGTCAGACCCCGTAGAAA, this primer is designed on pUC Ori sequence), and the buffer supplied by the manufacturer.
2. Set the first mixture to PCR thermocycler for 4 min denaturation at 94°C followed by 30 cycles of amplification: 98°C for 10 s, 55°C for 30 s, and 72°C for 5 min depending on the length of gene (1 kb per min).
3. Prepare 50 μL of a second PCR reaction mixture by mixing 5 μL of the first PCR product (without any purification) above as template, 200 μM each of dNTP, 1.5 units of ExTaq DNA polymerase, 100 nM SPu primer (5′-GCGTAG CATTTAGGTGACACT), 100 nM AODA2303 primer (5′-GTCAGACCCCGTAGAAAAGA, this primer is designed on pUC Ori sequence), and 2 nM DBtag fragment and the buffer supplied by the manufacturer.
4. Set the second PCR mixture to PCR thermocycler for 1 min denaturation at 98°C followed by 30 cycles of amplification: 98°C for 10 s, 55°C for 30 s, and 72°C for 5 min depending on the length of gene (1 kb per min).

5. Check the DNA template production by agarose electrophoresis (see Note 2).

3.2. DBtag Protein Production by Wheat Cell-Free System

We use bilayer method for protein production by the cell-free system (10). In principle, exchange of substrates and dilution of by-products take place between translation mix and TSB by expansion of translation mix.

3.2.1. Preparation of mRNA

1. Prepare 30 μL of transcription reaction by mixing 3 μL of the PCR mix (without any purification) as template, 6 μL of 5× TB, 3 μL of NTPs mix, 25 units of SP6 RNA polymerase, and 25 units of RNasin with Milli-Q water.
2. Incubate the reaction mixture at 37°C for 3 h.
3. Add 3 volumes of Milli-Q water, 1/7.5 vol. of 7.5 M ammonium acetate, and 2.5 vol. of ~99% EtOH, and keep on ice for 10 min after mixing well.
4. Centrifuge the mixture (20,000*g*; 5 min) and discard the supernatant.
5. Wash the pellet with 500 μL of 70% ethanol and then spin for 5 min at 20,000*g*.
6. Dissolve the mRNA pellet in 10 μL of Milli-Q water.

3.2.2. Preparation of DBtagged Proteins by Wheat Cell-Free Protein Production

1. Prepare 25 μL of translational reaction mixture by combining 6.3 μL of wheat embryo extract (final conc. 60 OD/mL), 1 μL of 10 mg/mL creatine kinase, 4.5 μL of 4× TSB, and 10 μL of the dissolved mRNA above.
2. Add 125 μL of 1× TSB in the U-shaped titer plate well.
3. Carefully place 25 μL of the reaction mixture at the bottom of titer plate well.
4. Place a coverlet on the plate and then wrap with the Saran Wrap to avoid evaporation.
5. Keep the plate in an incubator at 17°C for 16 h without shaking.

3.3. Generation of Protein Microarray Using DBtag Protein

We designed a new microplate that carries a thin layer of agarose gel containing DNA (agarose/DNA microplate) to immobilize and purify the DBtagged proteins on the microplate (Fig. 7.1b). Non-DBtagged proteins are washed out (Fig. 7.1c).

3.3.1. Preparation of Agarose/DNA Microplate

1. Melt 0.2% agarose gel in 1× TMD buffer, and subsequently add 1 mg/mL (final concentration) salmon sperm DNA.
2. Before the gel is solidified, spread 600 or 400 μL of the agarose gel/DNA mixture above on a slide glass or a Lab-Tek II Chamber slide, respectively, to form a thin layer (0.5–0.6 mm) (see Note 3).

3.3.2. Preparation of Protein Microarray on Agarose/DNA Microplate

1. Spot approximately 10 nL of each translational mixture per 0.2 mm^2 (~500 μm in diameter) on the agarose/DNA-coated glass plate by using pin-type spotter according to the instruction manual (see Note 4).
2. Soak the microplate in the wash buffer for 15 min.
3. Use immediately for assay (see Note 5).

3.4. Functional Analysis of DBtagged Protein on Agarose/DNA Microplate (see Note 5*)*

Using this new protein microarray, we demonstrate (a) the autophosphorylation activity of the fusion human protein kinases (Subheading 3.4.1. and Fig. 7.2a), (b) a protein–protein interaction between UBE2N (Accession no. NM_003348, MGC5063) and UBE2v1 (NM_022442, MGC8586) (Subheading 3.4.2. and Fig. 7.2b), and (c) specific cleavage of the fusion proteins (PAK2, NM_002577) by caspase 3 (Subheading 3.4.3. and Fig. 7.2c).

3.4.1. Inhibition Assay of DBtagged Protein Kinases on Agarose/DNA Microplate

1. Prepare the protein microarray spotting DBtag-fusion protein kinases on the agarose/DNA-coated glass plate as described above.
2. Cover the microplate with a kination solution or inhibitor solution.
3. Incubate for 30 min at 37°C.
4. Soak the microplate in washing buffer for 10 min.
5. Analyze the microplate by Typhoon 9400 imaging system.

3.4.2. Protein–Protein Interaction Analysis Between DBtagged Protein and Biotinylated Protein on Agarose/DNA Microplate

1. Prepare DBtag-UBE2N and biotinylated bls-UBE2V1 proteins by the cell-free system.
2. Mix both proteins with Alexa488-STA (final 10 μg/mL).
3. Incubate for 30 min at 26°C.
4. Spot the mixture on the agarose/DNA-coated glass plate as described above (Subheading 3.3.).
5. Soak the microplate in 1× PBS buffer for 10 min (see Note 6).
6. Analyze the microplate by Typhoon 9400 imaging system.

3.4.3. Caspase Cleavage Assay of DBtagged Proteins on Agarose/DNA Microplate

1. Prepare biotinylated substrate proteins (DBtag-PAK2-bls) by the cell-free system.
2. Mix the biotinylated proteins with Alexa488-STA (final 10 μg/ml).
3. Incubate for 30 min at 26°C.
4. Spot the mixture on the agarose/DNA-coated glass plate as described above (Subheading 3.3.).
5. Cover the microplate with caspase-3 solution.
6. Incubate for 30 min at 26°C.

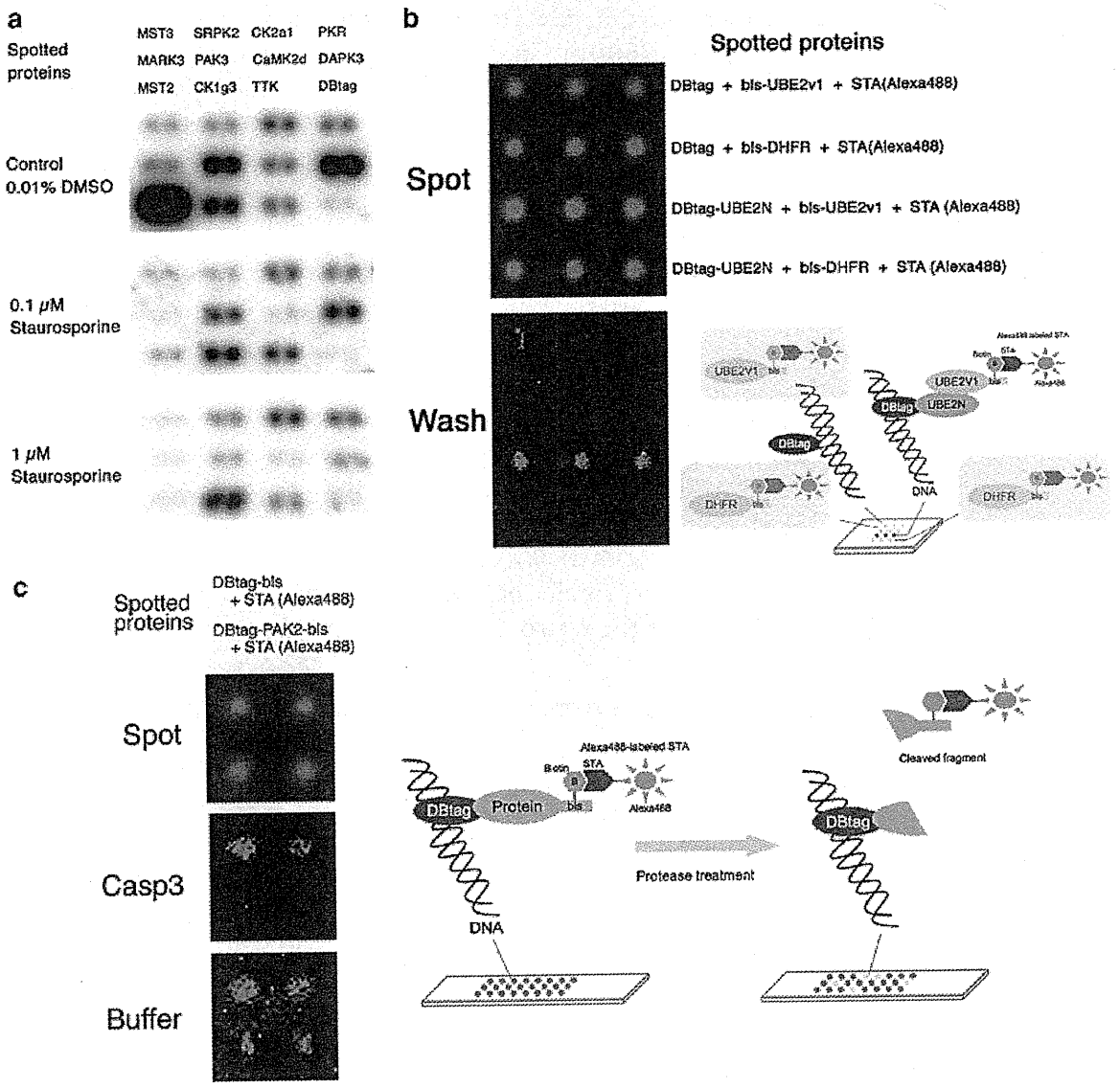

Fig. 7.2. (**a**) Detection and specific inhibition of the autophosphorylation activity of 11 human protein kinases on agarose/DNA microplate. The DBtagged human protein kinases were analyzed in duplicates. "DBtag" indicates the tag protein by itself (control). (**b**) Detection of a protein–protein interaction between UBE2N and UBE2v1 on the agarose/DNA microplate. Four samples (DBtag + biotin-labeled bls-UBE2v1 + STA(Alexa488), DBtag + biotin-labeled bls-DHFR + STA(Alexa488), DBtag-UBE2N + the bls-UBE2v1 + STA(Alexa488) and DBtag-UBE2N + the bls-DHFR + STA(Alexa488) from the top in "spot" panel] were spotted with three spots on the microplate. The first, second, and fourth samples lost the fluorescence after washing ("wash" panel). The third sample showed the fluorescence in "wash" panel, indicating a heterodimer as a protein–protein interaction between UBE2N and UBE2v1 proteins. An image from this result was shown in the *right panel.* (**c**) Two proteins including PAK2 (*lower spots* in each panel: DBtag-PAK2-bls labeled with Alexa488-STA) lost the fluorescence after the caspase 3 (casp3) treatment ("Casp3" panel). DBtag-bls proteins (*upper spots* in each panel: DBtag-bls labeled with Alexa488-STA) and buffer without the casp3 ("buffer" panel) showed fluorescence because they were not recognized by the casp3. *Right panel* indicates the schematic that the fluorescence-labeled region is released by the protease cleavage, and as a result, the fluorescence was lost upon washing.

7. Soak the microplate in 1× PBS buffer for 10 min (see Note 6).
8. Analyze the microplate by Typhoon 9400 imaging system.

4. Notes

1. Exonuclease I degrades extra primers after the PCR reaction. We often found primer contaminant in samples after Purification kit. The exonuclease I is very convenient to remove the extra primers because it is inactivated by simple heat treatment.
2. If DNA template is of low production, increase of primer concentration could provide higher production. In our case, the concentration increases to 100 nM from 10 nM as final concentration.
3. The agarose/slide-coated glass should be used within 1 day.
4. During spotting process, humidity inside the spotter should be kept. MultiSPRinter™ spotter can control high-humidity condition.
5. During making of the microplate and the assay, the microplate should be kept in a Tupperware box containing wet papers to prevent it from drying. Dried microplate could not be used for the functional analysis of proteins.
6. If soaking time is too long, assay sensitivity is decreased.

Acknowledgements

We greatly thank Satoko Matsunaga, Yuko Matsubara, Yoshiko Kodani, Yoshinori Tanaka, and two researchers (Mihoro Saeki and Dr. Ryo Morishita) working in CellFree Sciences Co., Ltd for their expert technical assistance. This work was partially supported by the Special Coordination Funds for Promoting Science and Technology by the Ministry of Education, Culture, Sports, Science and Technology, Japan.

References

1. Qin, S., Qiu, W., Ehrlich, J.R., Ferdinand, A.S., Richie, J.P., O'Leary M.P., Lee, M.L. and Liu, B.C. (2006) Development of a "reverse capture" autoantibody microarray for studies of antigen-autoantibody profiling. *Proteomics* **6**, 3199–3209.
2. Sheridan, C. (2005) Protein chip companies turn to biomarkers. *Nat. Biotechnol.* **23**, 3–4.
3. Zhu, H. and Snyder, M. (2003) Protein chip technology. *Curr. Opin. Chem. Biol.* **7**, 55–63.
4. Sawasaki, T., Ogasawara, T., Morishita, R. and Endo, Y. (2002) A cell-free protein

synthesis system for high-throughput proteomics. *Proc. Natl. Acad. Sci. USA.* **99,** 14652–14657.

5. Endo, Y. and Sawasaki, T. (2006) Cell-free expression systems for eukaryotic protein production. *Curr. Opin. Biotechnol.* **17,** 373–380.
6. Sawasaki, T., Gouda, M.D., Kawasaki, T., Tsuboi, T., Tozawa, Y., Takai, K. and Endo, Y. (2005) The wheat germ cell-free expression system: methods for high-throughput materialization of genetic information. *Methods Mol. Biol.* **310,** 131–144.
7. Sawasaki, T., Kamura, N., Matsunaga, S., Saeki, M., Tsuchimochi, M., Morishita, R. and Endo, Y. (2008) Arabidopsis HY5 protein functions as a DNA-binding tag for purification and functional immobilization of proteins on agarose/DNA microplate. *FEBS Lett.* **582,** 221–228.
8. Oyama, T., Shimura, Y. and Okada, K. (1997) The Arabidopsis HY5 gene encodes a bZIP protein that regulates stimulus-induced development of root and hypocotyl. *Genes Dev.* **11,** 2983–2995.
9. Kamura, N., Sawasaki, T., Kasahara, Y., Takai, K. and Endo, Y. (2005) Selection of 5′-untranslated sequences that enhance initiation of translation in a cell-free protein synthesis system from wheat embryos. *Bioorg. Med. Chem. Lett.* **15,** 5402–5406.
10. Sawasaki, T., Hasegawa, Y., Tsuchimochi, M., Kamura, N., Ogasawara, T. and Endo, Y (2002) A bilayer cell-free protein synthesis system for high-throughput screening of gene products. *FEBS Lett.* **514,** 102–105.

Vaccine 29 (2011) 2720–2726

Contents lists available at ScienceDirect

Vaccine

journal homepage: www.elsevier.com/locate/vaccine

Adenovirus-vectored *Plasmodium vivax* ookinete surface protein, Pvs25, as a potential transmission-blocking vaccine

Takeshi Miyata[a], Tetsuya Harakuni[a], Hideki Sugawa[a,b], Jetsumon Sattabongkot[c], Aki Kato[d], Mayumi Tachibana[e], Motomi Torii[e], Takafumi Tsuboi[d], Takeshi Arakawa[a,f,*]

[a] *Molecular Microbiology Group, Department of Tropical Infectious Diseases, COMB, Tropical Biosphere Research Center, University of the Ryukyus, 1 Senbaru, Nishihara, Okinawa 903-0213, Japan*
[b] *AMBiS Corporation, 2013 Ozato, Nanjyo, Okinawa 901-1202, Japan*
[c] *Department of Entomology, Armed Forces Research Institute of Medical Sciences, Bangkok 10400, Thailand*
[d] *Cell-Free Science and Technology Research Center, Ehime University, 3 Bunkyo-cho, Matsuyama, Ehime 790-8577, Japan*
[e] *Department of Molecular Parasitology, Ehime University, Graduate School of Medicine, Shitsukawa, Toon, Ehime 791-0295, Japan*
[f] *Division of Host Defense and Vaccinology, Graduate School of Medicine, University of the Ryukyus, 207 Uehara, Nishihara, Okinawa 903-0215, Japan*

ARTICLE INFO

Article history:
Received 10 September 2010
Received in revised form
29 December 2010
Accepted 21 January 2011
Available online 11 February 2011

Keywords:
Malaria transmission-blocking vaccine
Human adenovirus

ABSTRACT

Adjuvants or delivery vehicles are essential components to expedite malaria vaccine development. In this study, replication-defective human adenovirus serotype 5 (rAd) was genetically engineered to express the *Plasmodium vivax* ookinete surface protein (OSP), Pvs25 (AdPvs25). BALB/c mice immunized with the AdPvs25 through various routes including intramuscular, subcutaneous and intranasal routes were analyzed for induction of antigen-specific transmission-blocking immunity. Parenteral but not mucosal immunization induced high serum immunoglobulin G (IgG) responses specific to *P. vivax* ookinetes isolated from *P. vivax* volunteer patients from Thailand. The membrane feeding assay revealed that antisera conferred a transmission blockade of up to 99% reduction in the average oocyst numbers per mosquito, while immunization with a rAd expressing Pfs25 from *Plasmodium falciparum*, a homolog of Pvs25, conferred only a background level of blockade, suggesting that a species-specific transmission-blocking immunity was induced. Vaccine efficacy of AdPvs25 was slightly higher than to a recombinant Pvs25 protein mixed with aluminum hydroxide, but less efficacious than the protein emulsified with incomplete Freund's adjuvant. This study, the first preclinical evaluation of adenovirus-vectored malaria OSPs, implicates a potential inclusion of malaria transmission-blocking vaccine antigens in viral vector systems.

1. Introduction

Malaria is one of the most serious infectious diseases with high mortality and morbidity in large areas of tropical regions of the world. There were estimated 189–327 million cases and 881,000 malaria deaths in 2006 [1]. The majority of victims of malaria are children in sub-Saharan Africa. Implementation of various control measures including drug therapy and insecticide-treated bednets have made a substantial contribution to reduction of malaria cases over the past decades; however, these control measures are not sufficient partly due to the emergence of parasites resistant to antimalarial drugs and mosquito strains resistant to insecticides, and hence new prevention tools need to be developed for local elimination and the ultimate eradication of the disease [2–4]. The development of effective and affordable vaccines is therefore believed to benefit global public health by closing the gap left by the current malaria intervention measures [5].

Several promising vaccine candidates have been intensively investigated [6,7], such as those targeting sporozoite [8], hepatic and erythrocytic stages [9], which are designed to prevent infection and to reduce disease severity. On the other hand, transmission-blocking vaccines (TBVs) that target the sexual stage, in which the parasite undergoes sporogonic development in anopheline mosquitoes, prevent parasite transmission in the mosquito [10–12]. TBVs induce antibodies that react with the ookinete surface proteins (OSPs) of malaria parasites within the mosquito midgut, and as such they do not directly protect vaccinated individuals from infection. They could however contribute to elimination of the disease by lowering the parasite transmission

* Corresponding author at: Molecular Microbiology Group, Department of Tropical Infectious Diseases, COMB, Tropical Biosphere Research Center, University of the Ryukyus, 1 Senbaru, Nishihara, Okinawa 903-0213, Japan.
Tel.: +81 98 895 8974; fax: +81 98 895 8974.
E-mail address: tarakawa@comb.u-ryukyu.ac.jp (T. Arakawa).

0264-410X/$ – see front matter © 2011 Elsevier Ltd. All rights reserved.
doi:10.1016/j.vaccine.2011.01.083

frequency below the threshold at which the parasite can maintain its life cycle [2,13,14]. Additionally, TBVs, if combined with vaccines targeting other infection stages, could prevent transmission of escape mutants that emerge during infection. Therefore, TBVs might function as a "safety net" for pre-erythrocytic and erythrocytic vaccines, as well as other non-vaccine interventions.

Plasmodium falciparum causes the highest mortality rates among the four *Plasmodium* species known to infect humans; however *Plasmodium vivax*, the second most prevalent malaria species, causes 80–300 million clinical cases every year [15], has the highest morbidity and is a major cause of recurrent malaria. Its clinical manifestations range from asymptomatic to severe diseases that in some cases lead to death. Additionally, an increase in the number of severe cases of *P. vivax* infection casts doubts regarding what was thought to be its relatively benign nature [16]. This species is therefore an important target of malaria control efforts [5,13–15,17]. Furthermore, because global malaria eradication is the ultimate goal, the value of developing vaccines against *P. vivax* can no longer be underestimated [5,13–15,17].

The majority of malaria vaccine candidate antigens currently under preclinical and clinical evaluation are recombinant in origin [6,7], and therefore they are only marginally immunogenic by themselves. This has been demonstrated to be true for the two *P. vivax* candidate vaccine antigens recently tested in clinical trials, the circumsporozoite protein (CSP) [13,18] and Pvs25 OSP [13,19,20]. Therefore, appropriate adjuvant formulations or employment of delivery systems seem to be extremely important in inducing an optimal antiparasite immune response.

Replication-defective human adenovirus has been intensively evaluated for the delivery of foreign genes in gene therapy and for vaccine development against infectious diseases including malaria [21–23]. The ability to induce both cell-mediated and humoral immunities as well as a long-lasting memory T cell response are generally considered advantages of the viral vector systems in vaccine development against malaria [21,23,24]. Those immunities are important to confer solid protection against infection [25]. Attenuated adenovirus has been used for US military recruits to prevent respiratory infection [23,26], therefore safety issues may not be a serious concern for this viral vector system. *P. falciparum* antigens at the pre-erythrocytic stage such as CSP and liver-stage antigen-1 (LSA1), and antigens at the erythrocytic stage such as apical membrane antigen-1 (AMA1) and merozoite surface protein-1 (MSP1) are being tested in clinical trials as adenovirus-vectored antigens [7,23].

Since TBVs require efficient antibody-inducing capacity [10–12,27–30], we therefore hypothesized that the adenovirus vector system is beneficial for this purpose. In this study we evaluated potential application of a replication-defective human adenovirus serotype 5 to induce transmission-blocking immunity against *P. vivax* malaria. The vaccine efficacy of the induced mouse antisera was evaluated by a membrane-feeding assay using field strains of parasites obtained from *P. vivax* volunteer patients in Thailand.

2. Materials and methods

2.1. Immunization with a recombinant adenovirus expressing Pvs25

AdPvs25 is a replication-defective human adenovirus serotype 5, expressing the Pvs25 gene under the regulation of the cytomegalovirus enhancer and promoter [31]. Genetic engineering of AdPvs25 was conducted based on a COS-TPC method, according to the manufacturer's instructions (TAKARA Bio, Otsu, Japan). Recombinant Pvs25 (rPvs25) protein expressed and purified from the methylotrophic yeast *Pichia pastoris* [27] was used to comparatively evaluate immunogenicity of AdPvs25.

Eight-week-old female BALB/c mice were purchased from Japan SLC (Shizuoka, Japan), and housed in a special pathogen-free environment in our research institute. Mice were immunized four times at weeks 0, 3, 5 and 7 *via* subcutaneous (s.c.; 100 μl at a single injection site), intramuscular (i.m.; 50 μl at two injection sites), intranasal (i.n.; 15 μl into each nostril), or intragastric (i.g.; 200 μl) route with 5.1×10^9 plaque forming units/ml of AdPvs25, or three times at weeks 0, 2 and 4 *via* the s.c. route with 30 μg of the rPvs25 protein alone, or with incomplete Freund's adjuvant (IFA; Difco Laboratories, Detroit, MI, USA) or aluminum hydroxide (Alum; Pierce, Rockford, IL, USA) as controls.

All animal experimental protocols used in this study were approved by the Institutional Animal Care and Use Committee of the University of the Ryukyus, and the experiments were conducted according to the Ethical Guidelines for Animal Experiments of the University of the Ryukyus.

2.2. ELISA for antibody titer determination

Mouse antisera were collected 1–2 weeks after the last immunization (week 8 or 6 for AdPvs25 or rPvs25 protein, respectively), and Pvs25-specific serum IgG was analyzed by ELISA as described previously [27–30]. Briefly, the ELISA plates (Sumilon; Sumitomo Bakelite Co., Ltd., Tokyo, Japan) were coated with 5 μg/ml of rPvs25 in bicarbonate buffer overnight at 4 °C and blocked with 1% (w/v) bovine serum albumin (BSA) in phosphate buffered saline (PBS) for 2 h at 37 °C. Two-fold serial dilutions of the antisera, commencing with an initial 50-fold dilution with 0.5% (w/v) BSA in PBS, were applied to wells (2 h, 37 °C). Anti-mouse IgG conjugated to alkaline phosphatase (1/4000; Sigma–Aldrich, St. Louis, MO, USA) was added to the wells and incubated for 2 h at 37 °C, before its substrate *p*-nitrophenylphosphate (Bio-Rad Laboratories, Inc., Redmond, WA, USA) was applied for 20 min at 37 °C and the absorbance at 415 nm (OD_{415}) was read on a microplate reader (Bio-Rad). The plates were washed twice with PBS containing 0.05% Tween-20 (PBS-T) and once with PBS between each incubation step. The antibody titer was defined as the serum dilution that gave an OD_{415} value equal to 0.1, or as the serum dilution where a one magnitude higher dilution gave an OD_{415} value less than 0.1.

2.3. Mosquito membrane feeding assay

The membrane feeding assay was conducted as described previously [27–29]. Briefly, peripheral blood was collected, with written informed consent, from *P. vivax* volunteer patients who came to a malaria clinic in the Mae Sod district in the Tak province of northwestern Thailand. Plasma was removed from the collected blood. Single species infection with *P. vivax* was confirmed by Giemsa stain prior to the assay. The vaccine-induced mouse antisera were mixed with an equal volume of heat-inactivated human AB serum obtained from malaria-naïve volunteers. Then, the mouse antisera and the human AB serum mixture was added to the parasitized blood cells obtained from the patients (1:1 v/v ratio), and incubated for 15 min at room temperature. The mixture was applied to a membrane feeding apparatus kept at 37 °C to feed *Anopheles dirus* A mosquitoes (Bangkok colony, Armed Forces Research Institute of Medical Sciences) for 30 min. Fully engorged mosquitoes were maintained for a week in an insectary kept at 26 °C. For each test sample, 20 mosquitoes were analyzed to count the number of oocysts that had developed in the midgut.

Human subject research conducted in this study was reviewed and approved by the Ethics Committee of the Thai Ministry of Public Health and the Institutional Review Board of the Walter Reed Army Institute of Research.

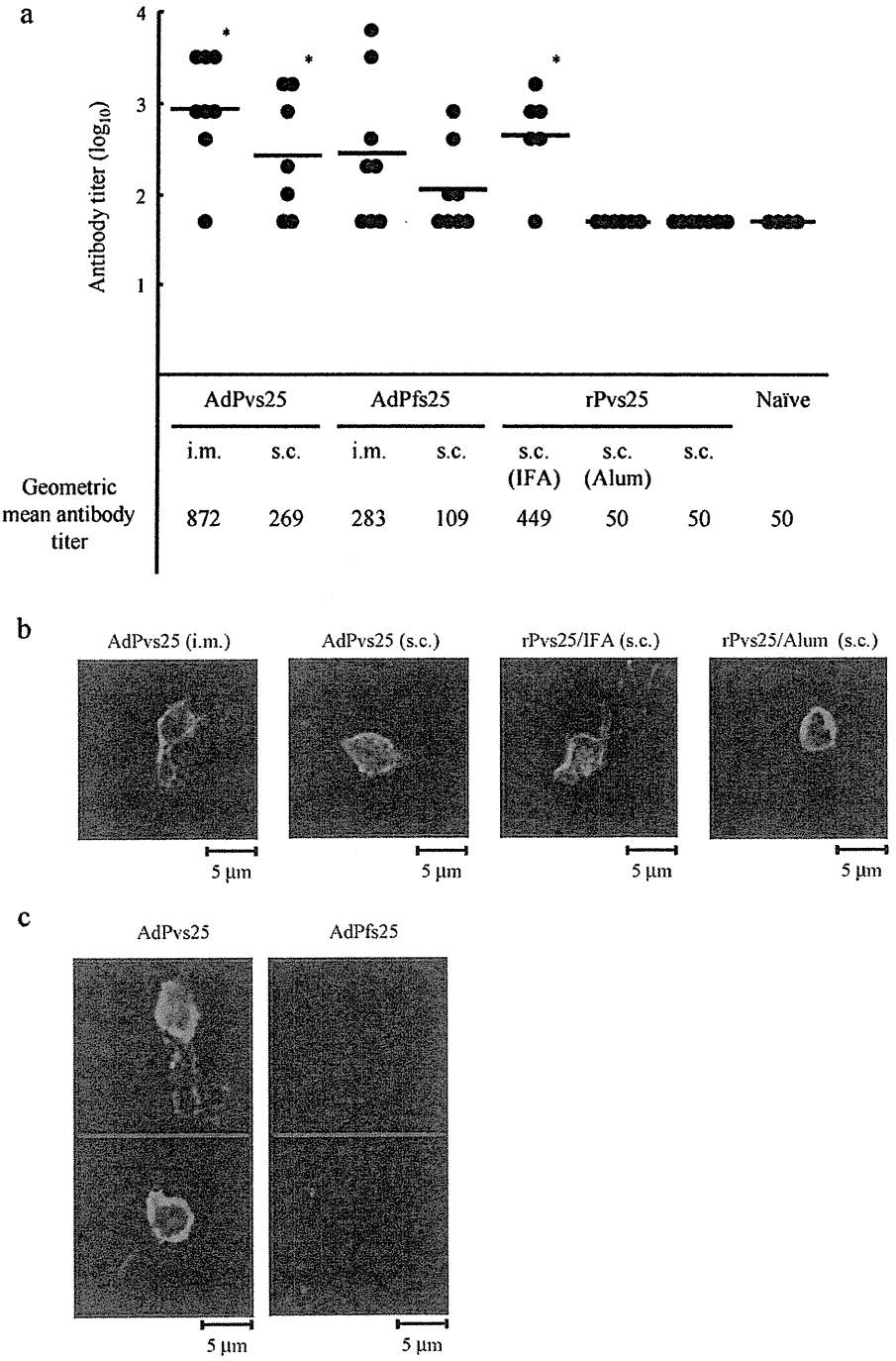

Fig. 1. Immunogenicity of AdPvs25 in mice. (a) Eight-week-old female BALB/c mice were immunized four times at weeks 0, 3, 5 and 7 *via* subcutaneous (s.c.) or intramuscular (i.m.) route with 5.1×10^8 plaque forming units of the AdPvs25, or three times at weeks 0, 2 and 4 *via* the s.c. route with 30 μg of recombinant Pvs25 (rPvs25) protein alone, or with incomplete Freund's adjuvant (IFA) or aluminum hydroxide (Alum), as controls. Serum samples were collected at week 8 or 6 for the adenovirus-vectored or the recombinant protein immunization, respectively, and evaluated for Pvs25-specific IgG titers. Serum from naïve mice was used as a negative control for the ELISA. Antibody titers were defined as the serum dilution that resulted in an OD_{415} of 0.1, or as the serum dilution where a one magnitude higher dilution gave an OD_{415} value less than 0.1. * indicates a significant difference to non-immune serum by the Wilcoxon–Mann–Whitney test ($P<0.05$). (b) Ookinete-specific reactivity of the induced antisera as analyzed by immunofluorescence. The antisera derived from i.m. or s.c. immunization with the AdPvs25, or s.c. immunization with the rPvs25 protein emulsified with IFA or the rPvs25 protein mixed with Alum specifically recognized native Pvs25 protein expressed on the surface of *P. vivax* zygote/immature ookinetes. (c) The antisera derived from i.m. immunization with the AdPvs25 or the AdPfs25 were reacted to *P. vivax* zygote/immature ookinetes, indicating the specificity of the AdPvs25 antisera.

2.4. Detection of native Pvs25 using mouse antisera

Peripheral blood of *P. vivax*-infected volunteer patients was collected as described above. The gametocytemic blood was used to grow zygotes and ookinetes *in vitro* [32], then samples were spotted onto slides and fixed with acetone as described previously [27–30]. The slides were then blocked with 5% nonfat milk in PBS, and incubated with the mouse antiserum derived from immunization with

the AdPvs25, AdPfs25, or the rPvs25 protein emulsified with IFA, or the rPvs25 protein mixed with Alum, after diluting the antisera 100-fold with 5% nonfat milk in PBS. The samples were washed with ice-cold PBS and incubated with Alexa488-conjugated anti-mouse antibody (Invitrogen, Carlsbad, CA, USA). After washing with ice-cold PBS, slides were viewed by confocal scanning laser microscopy (LSM5 PASCAL; Carl Zeiss MicroImaging, Thornwood, NY, USA).

2.5. Statistical analysis

Statistical analyses were conducted by the Wilcoxon–Mann–Whitney test or the Kruskal–Wallis test using JMP software version 8.0 (SAS Institute, Inc., Cary, NC, USA).

3. Results and discussion

There is an increasing demand for the development of effective recombinant vaccine platform technologies to enhance vaccine efficacy by the innovation of new adjuvants or delivery systems [33]. This would seem to be particularly true for OSPs, because they are low-molecular-weight proteins that are by themselves not sufficiently immunogenic.

In this study, we engineered replication-defective human adenovirus serotype 5 for expression of a *P. vivax* OSP, Pvs25, to test its efficacy to induce transmission-blocking immunity. We immunized BALB/c mice through various routes including i.m., s.c., i.n. and i.g., and the Pvs25-specific serum IgG response was measured (Fig. 1a and Table 1). Parenteral (i.m. and s.c.) but not mucosal (i.n. and i.g.) immunization (Supplementary data Fig. 1) with the AdPvs25 induced robust IgG responses comparable in titers to those induced by the rPvs25 protein administered s.c. with IFA. Immunization by the i.m. route with the AdPvs25 tended to induce higher IgG response than s.c. immunization, and at least three booster injections seemed to be necessary to induce the maximal level of response (Supplementary data Fig. 1). AdPvs25-induced antisera could efficiently recognize the *P. vivax* ookinete surface as determined by the immunofluorescence assay (Fig. 1b). Although, rPvs25 protein immunization with aluminum hydroxide induced only a background level of IgG response as compared with the unimmunized naïve control serum (Fig. 1a), the induced antiserum could recognize the parasite surface as efficiently as the AdPvs25 or the rPvs25/IFA induced antiserum (Fig. 1b).

AdPfs25 immunization, particularly for the i.m. route, induced relatively high IgG response to the rPvs25 protein as determined by ELISA (Fig. 1a and Supplementary data Fig. 2), implicating that the induced antisera are somewhat cross-reactive at least at the recombinant protein level; however, the differences in IgG titers between AdPfs25 and the unimmunized naïve control groups did not reach statistically significant levels. Further, AdPfs25 antisera failed to react to the *P. vivax* ookinete (Fig. 1c), indicating the specificity of the AdPvs25 antisera.

Next, we evaluated the TBV efficacy of the induced mouse antisera against field isolates of *P. vivax* parasites in infected blood samples from volunteer patients in Thailand by the membrane feeding assay as described previously [28,29]. The same experiments were performed three times using blood samples from three different *P. vivax* (Pv)-infected volunteer donors (Pv-infected blood donors 1–3; Fig. 2a–c and Table 1). The average number of oocysts per mosquito fed on parasitized blood mixed with the antisera induced by parenteral immunization (i.m. or s.c.) with the AdPvs25 was reduced by 82–99% as compared with the unimmunized naïve control serum when parasite burden was low (Fig. 2a and b and Table 1). Although, the rPvs25/Alum induced no detectable Pvs25-specific serum IgG response (Fig. 1a and Table 1), its TBV efficacy (92–97% blockade; Fig. 2a and b and Table 1) was com-

Table 1
Summary of immunization experiments outlining antibody titers and transmission-blocking effects.

Immunization group	Immunization route	Adjuvant	Geometric mean antibody titer	TBV effect (Pv-infected blood donor 1)		TBV effect (Pv-infected blood donor 2)		TBV effect (Pv-infected blood donor 3)	
				Average oocyst number per mosquito (median oocyst number)	% Reduction in average oocyst number per mosquito (oocyst-free mosquitoes per 20 mosquitoes)	Average oocyst number per mosquito (median oocyst number)	% Reduction in average oocyst number per mosquito (oocyst-free mosquitoes per 20 mosquitoes)	Average oocyst number per mosquito (median oocyst number)	% Reduction in average oocyst number per mosquito (oocyst-free mosquitoes per 20 mosquitoes)
AdPvs25	i.m.	–	872§	1.5* (1.0)	82.3 (9)	0.1* (0)	98.6 (19)	10.0* (3.0)	71.4 (7)
	s.c.	–	269§	1.0* (0)	87.8 (11)	1.3* (0)	82.4 (13)	25.0 (14.5)	28.5 (1)
AdPfs25	i.m.	–	283	10.0 (7.0)	0 (4)	5.5 (5.0)	25.7 (3)	85.3 (71.5)	0 (0)
	s.c.	–	109	16.6 (18.0)	0 (1)	7.9 (6.0)	0 (1)	207.3 (206.0)	0 (0)
rPvs25	s.c.	IFA	449§	0* (0)	100 (20)	0* (0)	100 (20)	0* (0)	100 (20)
	s.c.	Alum	50	0.7* (0)	91.5 (13)	0.2* (0)	97.3 (17)	31.2 (24.5)	10.9 (1)
	s.c.	–	50	7.0 (6.0)	14.6 (1)	1.4* (0.5)	81.1 (10)	53.5 (34.0)	0 (1)
Naïve		–	50	8.2 (7.5)	0 (3)	7.4 (4.5)	0 (5)	35.0 (14.5)	0 (0)

i.m.: intramuscular; s.c.: subcutaneous; IFA: incomplete Freund's adjuvant; Alum: aluminum hydroxide; TBV: transmission-blocking vaccine; Pv: *Plasmodium vivax*.
* $P < 0.001$ vs. naïve.
§ $P < 0.005$ vs. naïve.
% Reduction is calculated as the reduction in the average oocyst number for each immunization group compared to the average oocyst number for the unimmunized naïve control group.

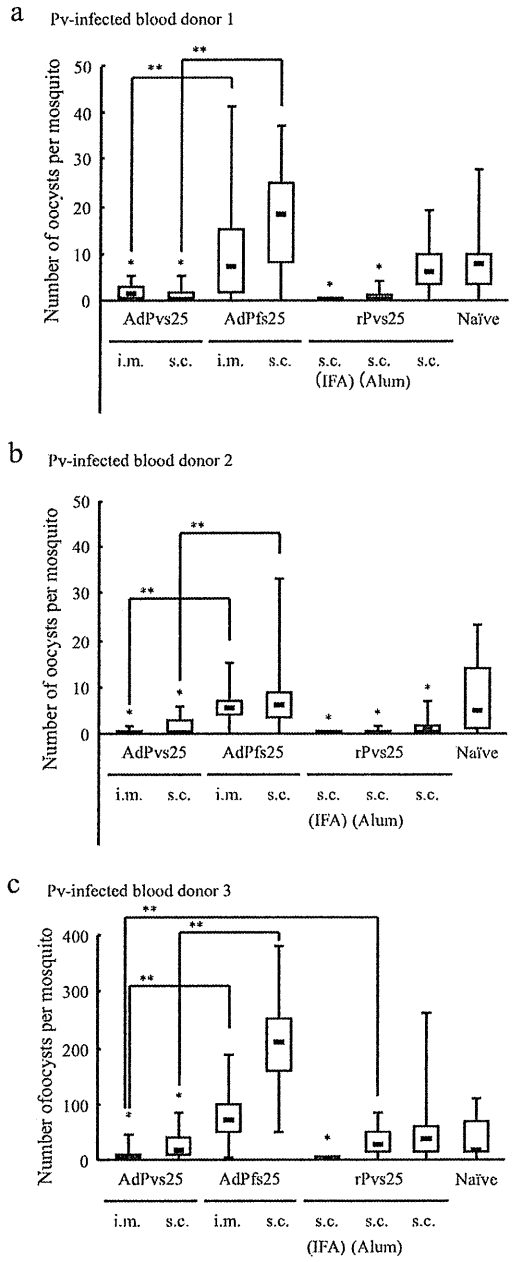

Fig. 2. Transmission-blocking effects induced by antisera (1/2 dilution) derived from mice immunized with the AdPvs25, the AdPfs25, or the rPvs25 protein were evaluated. The data were expressed as the median values of oocyst number per mosquito (black bar within the box) with 25% and 75% quartiles (box) and ranges (error bars). Three independent experiments were performed, using three blood samples from Pv-infected blood donors 1–3. * $P<0.001$ *vs.* naïve mice by the Wilcoxon–Mann–Whitney test; ** $P<0.001$ between the indicated two groups by the Wilcoxon–Mann–Whitney test.

parable to those attained by the AdPvs25. We do not know why the rPvs25/Alum immunization conferred substantial TBV efficacy without inducing antibody response detectable in ELISA (Fig. 1a); however, when the level of parasite burden increased as seen in the case for donor 3, the AdPvs25 appeared to become significantly more efficacious than the rPvs25/Alum, particularly for the i.m. immunization regimen (Fig. 2c and Table 1). These results suggest that adenovirus-vectored Pvs25 has potentially higher vaccine efficacy than the Alum-adjuvanted rPvs25 protein.

The rPvs25/IFA immunization consistently conferred a complete blockade regardless of the level of parasite burden; however, the local reactogenicity was considerably higher than Alum-adjuvanted or adenovirus-vectored immunization regimen.

Intraperitoneal or intravenous immunization with the AdPvs25 induced a robust serum IgG response, although its TBV effect was not assessed in this study. In contrast, despite the fact that adenoviruses mainly affect the respiratory system, the AdPvs25 administered by the i.n. route failed to induce a specific serum IgG response as determined by the ELISA (Supplementary Fig. 1). This might be due to the fact that only a low virus dose was able to be administered. However, the rPvs25 protein administered i.n. with a minute amount of cholera toxin (CT) adjuvant consistently induced a strong IgG response in mice, and as such its level of efficacy was very similar to that attained by the i.m. administered AdPvs25 immunization regimen (data not shown). Thus, it seems that adenovirus-vectored i.n. immunization is much less effective than the recombinant protein antigen administered through the same route with a potent mucosal adjuvant like CT. Administration through the i.g. route was also tested in this study, but failed to induce any antibody response, probably because the gastrointestinal environment is too destructive for the virus to effectively transduce the foreign gene. The intravaginal route was found to be another ineffective route to induce an antibody response by adenovirus immunization, and as such no specific serum IgG was observed. The reason for this failure might be the same as those for i.n. immunization.

In this study we concomitantly engineered a replication-defective adenovirus expressing Pfs25, an ortholog gene of Pvs25. Its immunization induced low but detectable cross-reactive serum IgG to the rPvs25 protein, although it did not reach a level of statistical significance as compared with the naïve control serum (Fig. 1a). However, the membrane feeding assay confirmed that no TBV effect was induced against *P. vivax* species (Fig. 2), suggesting that induction of interspecies cross-blocking immunity cannot be expected. However, a mixed administration of the two adenovirus vectors each expressing Pfs25 and Pvs25, or engineering of a single virus vector that co-expresses both P25 genes should be technically feasible, implicating that multi-species TBVs could be constructed. To address this possibility, we conducted a preliminary immunization experiment in which a mixture of the two adenoviruses, AdPfs25 and AdPvs25, were administered through various routes, and assessed immunogenicity towards both proteins. The results implicated that the existence of multiple viral vectors did not have a negative impact on the induction of specific IgG responses against the individual protein (data not shown).

Heterologous prime–boost regimens employing different viral vectors, different administration routes, or different vaccine formulations such as those using plasmid DNA or recombinant proteins, is thought to be a promising approach to enhance vaccine efficacy of malaria antigens [23,34–38]. To determine whether the prime–boost regimen is also applicable to OSP-based TBVs, we tested a DNA prime-adenovirus vector boost (one DNA injection and three consecutive adenovirus injections). The results implicated however that DNA immunization does not adequately replace adenovirus vector immunization, because the level of antibody remained lower than the adenovirus vector only immunization regimen (data not shown). Similarly, a combination of different immunization routes was evaluated and from our results, we concluded that replacement of parenteral with mucosal immunization induced a lower immune response (data not shown). Taken together, these results implicate that DNA or mucosal immunization, which was by itself found not to be sufficiently immunogenic, when combined with the parenteral adenovirus vector immunization, ablated to varying degrees the

overall vaccine efficacy. However, we were unable to make a final conclusive statement, at this preliminary stage of evaluation, regarding the suitability of a prime–boost regimen and whether or not it could be applied for TBVs. This is because there are other various possible combinations that need to be tested, such as an adenovirus prime–vaccinia virus boost regimen, which is known to be one of the most effective combinations [36,38].

Since OSP-based TBVs do not directly protect vaccinated individuals from infection, it should not be used as a "standalone" malaria vaccine. Researchers are beginning to realize that a single antigen, a single stage, or even a single species malaria vaccine developmental strategy can no longer be considered as a practical or realistic strategy, as was previously believed [5], and therefore a combination of heterologous immunization regimens, including the prime–boost method, need to be pursued more vigorously for future malaria vaccine development. In this sense, it is very feasible and should be technically possible to combine adenovirus-vectored TBVs with other virus vectored vaccines, such as vaccinia virus, or with viral vectors targeting the pre-erythrocytic or erythrocytic stages of single or multiple malaria species, or even in combination with vaccines targeting other infectious diseases.

Of course, there is still much scope for optimizing adenovirus-vectored OSP-based TBVs. For example, adenovirus serotype 5 used in the present study may need to be changed to other serotypes for future clinical application in malaria endemic areas in Africa, because a large proportion of African population has high serotype 5 antibody [37]. However, the present study should at least support the notion that malaria OSP antigens can be included in adenovirus-vectored or possibly other viral vectored immunization regimens, and that they are able to induce comparable levels of humoral immunity compared with those induced by the recombinant proteins combined with the Alum adjuvant.

Acknowledgments

We thank the staff of the Armed Forces Research Institute of Medical Sciences in Bangkok, Thailand, for their technical assistance. This work was supported by grants from the Program of Founding Research Centers for Emerging and Reemerging Infectious Diseases from The Ministry of Education, Culture, Sports, Science and Technology, Japan (MEXT); Grants-in-Aid for Scientific Research (19406009 and 20590425) and Scientific Research on Priority Areas (21022034) from MEXT; a grant from the Okinawa Industry Promotion Public Corporation; and the Cooperative Research Grant of the Institute of Tropical Medicine, Nagasaki University.

Appendix A. Supplementary data

Supplementary data associated with this article can be found, in the online version, at doi:10.1016/j.vaccine.2011.01.083.

References

[1] WHO. World Health Report. 2008.
[2] Greenwood BM, Fidock DA, Kyle DE, Kappe SH, Alonso PL, Collins FH, et al. Malaria: progress, perils, and prospects for eradication. J Clin Invest 2008;118(4 (April)):1266–76.
[3] Targett GA, Greenwood BM. Malaria vaccines and their potential role in the elimination of malaria. Malar J 2008;7(Suppl. 1):S10.
[4] Genton B. Malaria vaccines: a toy for travelers or a tool for eradication? Expert Rev Vaccines 2008;7(5 (July)):597–611.
[5] PATH malaria vaccine initiative: about the malaria vaccine roadmap. Available from: http://www.malariavaccineorg/malvac-roadmap.php.
[6] Sharma S, Pathak S. Malaria vaccine: a current perspective. J Vector Borne Dis 2008;45(1 (March)):1–20.
[7] WHO. Malaria vaccine rainbow tables. Available from: http://www.who.int/vaccine_research/links/Rainbow/en/index.html.
[8] Ballou WR. The development of the RTS, S malaria vaccine candidate: challenges and lessons. Parasite Immunol 2009;31(9 (September)):492–500.
[9] Richards JS, Beeson JG. The future for blood-stage vaccines against malaria. Immunol Cell Biol 2009;87(5 (July)):377–90.
[10] Tsuboi T, Tachibana M, Kaneko O, Torii M. Transmission-blocking vaccine of *vivax* malaria. Parasitol Int 2003;52(1 (March)):1–11.
[11] Kaslow DC. Transmission-blocking vaccines: uses and current status of development. Int J Parasitol 1997;27(2 (February)):183–9.
[12] Carter R. Transmission blocking malaria vaccines. Vaccine 2001;19(17–19 (March)):2309–14.
[13] Arevalo-Herrera M, Chitnis C, Herrera S. Current status of *Plasmodium vivax* vaccine. Hum Vaccin 2010;6(1 (January)).
[14] Birkett AJ. PATH malaria vaccine initiative (MVI): perspectives on the status of malaria vaccine development. Hum vaccin 2010;6(1 (January)):139–45.
[15] Sina B. Focus on *Plasmodium vivax*. Trends Parasitol 2002;18(7 (July)):287–9.
[16] Kochar DK, Das A, Kochar SK, Saxena V, Sirohi P, Garg S, et al. Severe *Plasmodium vivax* malaria: a report on serial cases from Bikaner in northwestern India. Am J Trop Med Hyg 2009;80(2 (February)):194–8.
[17] Bill and Melinda Foundation. Global Health Program. Available from: http://www.gatesfoundation.org/global-health/Documents/malaria-strategy.pdf.
[18] Herrington DA, Nardin EH, Losonsky G, Bathurst IC, Barr PJ, Hollingdale MR, et al. Safety and immunogenicity of a recombinant sporozoite malaria vaccine against *Plasmodium vivax*. Am J Trop Med Hyg 1991;45(6 (December)):695–701.
[19] Malkin EM, Durbin AP, Diemert DJ, Sattabongkot J, Wu Y, Miura K, et al. Phase 1 vaccine trial of Pvs25H: a transmission blocking vaccine for *Plasmodium vivax* malaria. Vaccine 2005;23(24 (May)):3131–8.
[20] Wu Y, Ellis RD, Shaffer D, Fontes E, Malkin EM, Mahanty S, et al. Phase 1 trial of malaria transmission blocking vaccine candidates Pfs25 and Pvs25 formulated with montanide ISA 51. PLoS ONE 2008;3(7):e2636.
[21] Li S, Locke E, Bruder J, Clarke D, Doolan DL, Havenga MJ, et al. Viral vectors for malaria vaccine development. Vaccine 2007;25(14 (March)):2567–74.
[22] Draper SJ, Heeney JL. Viruses as vaccine vectors for infectious diseases and cancer. Nat Rev Microbiol 2010;8(1 (January)):62–73.
[23] Limbach KJ, Richie TL. Viral vectors in malaria vaccine development. Parasite Immunol 2009;31(9 (September)):501–19.
[24] Reyes-Sandoval A, Harty JT, Todryk SM. Viral vector vaccines make memory T cells against malaria. Immunology 2007;121(2 (June)):158–65.
[25] Beeson JG, Osier FH, Engwerda CR. Recent insights into humoral and cellular immune responses against malaria. Trends Parasitol 2008;24(12 (December)):578–84.
[26] Russell KL, Hawksworth AW, Ryan MA, Strickler J, Irvine M, Hansen CJ, et al. Vaccine-preventable adenoviral respiratory illness in US military recruits, 1999–2004. Vaccine 2006;24(15 (April)):2835–42.
[27] Miyata T, Harakuni T, Tsuboi T, Sattabongkot J, Kohama H, Tachibana M, et al. *Plasmodium vivax* ookinete surface protein, Pvs25, linked to cholera toxin B subunit induces potent transmission-blocking immunity by intranasal as well as subcutaneous immunization. Infect Immun 2010.
[28] Arakawa T, Komesu A, Otsuki H, Sattabongkot J, Udomsangpetch R, Matsumoto Y, et al. Nasal immunization with a malaria transmission-blocking vaccine candidate, Pfs25, induces complete protective immunity in mice against field isolates of *Plasmodium falciparum*. Infect Immun 2005;73(11 (November)):7375–80.
[29] Arakawa T, Tsuboi T, Kishimoto A, Sattabongkot J, Suwanabun N, Rungruang T, et al. Serum antibodies induced by intranasal immunization of mice with *Plasmodium vivax* Pvs25 co-administered with cholera toxin completely block parasite transmission to mosquitoes. Vaccine 2003;21(23 (July)):3143–8.
[30] Arakawa T, Tachibana M, Miyata T, Harakuni T, Kohama H, Matsumoto Y, et al. Malaria ookinete surface protein-based vaccination via the intranasal route completely blocks parasite transmission in both passive and active vaccination regimens in a rodent model of malaria infection. Infect Immun 2009;77(12 (December)):5496–500.
[31] Kass-Eisler A, Li K, Leinwand LA. Prospects for gene therapy with direct injection of polynucleotides. Ann NY Acad Sci 1995;772(November):232–40.
[32] Suwanabun N, Sattabongkot J, Tsuboi T, Torii M, Maneechai N, Rachapaew N, et al. Development of a method for the in vitro production of *Plasmodium vivax* ookinetes. J Parasitol 2001;87(4 (August)):928–30.
[33] O'Hagan DT, Valiante NM. Recent advances in the discovery and delivery of vaccine adjuvants. Nat Rev Drug Discov 2003;2(9 (September)):727–35.
[34] Kongkasuriyachai D, Bartels-Andrews L, Stowers A, Collins WE, Sullivan J, Sattabongkot J, et al. Potent immunogenicity of DNA vaccines encoding *Plasmodium vivax* transmission-blocking vaccine candidates Pvs25 and Pvs28-evaluation of homologous and heterologous antigen-delivery prime–boost strategy. Vaccine 2004;22(23–24 (August)):3205–13.
[35] Coban C, Philipp MT, Purcell JE, Keister DB, Okulate M, Martin DS, et al. Induction of *Plasmodium falciparum* transmission-blocking antibodies in nonhuman primates by a combination of DNA and protein immunizations. Infect Immun 2004;72(1 (January)):253–9.
[36] Reyes-Sandoval A, Berthoud T, Alder N, Siani L, Gilbert SC, Nicosia A, et al. Prime–boost immunization with adenoviral and modified vaccinia virus Ankara vectors enhances the durability and polyfunctionality of pro-

tective malaria CD8+ T-cell responses. Infect Immun 2010;78(1 (January)): 145–53.
[37] Hill AV, Reyes-Sandoval A, O'Hara G, Ewer K, Lawrie A, Goodman A, et al. Prime–boost vectored malaria vaccines: progress and prospects. Hum vaccin 2010;6(1 (January)).
[38] Bruna-Romero O, Gonzalez-Aseguinolaza G, Hafalla JC, Tsuji M, Nussenzweig RS. Complete, long-lasting protection against malaria of mice primed and boosted with two distinct viral vectors expressing the same plasmodial antigen. Proc Natl Acad Sci USA 2001;98(20 (September)):11491–6.

Parasitology International 60 (2011) 132–138

Contents lists available at ScienceDirect

Parasitology International

journal homepage: www.elsevier.com/locate/parint

Plasmodial ortholog of *Toxoplasma gondii* rhoptry neck protein 3 is localized to the rhoptry body

Daisuke Ito [a], Eun-Taek Han [b], Satoru Takeo [a], Amporn Thongkukiatkul [c], Hitoshi Otsuki [d], Motomi Torii [e], Takafumi Tsuboi [a,f,*]

[a] *Cell-Free Science and Technology Research Center, Ehime University, Matsuyama, Ehime 790-8577, Japan*
[b] *Department of Parasitology, Kangwon National University College of Medicine, Chuncheon, Republic of Korea*
[c] *Department of Biology, Faculty of Science, Burapha University, Chonburi 20131, Thailand*
[d] *Division of Medical Zoology, Faculty of Medicine, Tottori University, Yonago, Tottori 683-8503, Japan*
[e] *Department of Molecular Parasitology, Ehime University Graduate School of Medicine, Shitsukawa, Toon, Ehime 791-0295, Japan*
[f] *Venture Business Laboratory, Ehime University, Matsuyama, Ehime 790-8577, Japan*

ARTICLE INFO

Article history:
Received 23 November 2010
Received in revised form 24 December 2010
Accepted 7 January 2011
Available online 13 January 2011

Keywords:
Cell-free expression
Erythrocyte invasion
Merozoite
Plasmodium falciparum
Rhoptry

ABSTRACT

The proteins in apical organelles of *Plasmodium falciparum* merozoite play an important role in invasion into erythrocytes. Several rhoptry neck (RON) proteins have been identified in rhoptry proteome of the closely-related apicomplexan parasite, *Toxoplasma gondii*. Recently, three of *P. falciparum* proteins orthologous to *TgRON* proteins, *Pf*RON2, 4 and 5, were found to be located in the rhoptry neck and interact with the micronemal protein apical membrane antigen 1 (*Pf*AMA1) to form a moving junction complex that helps the invasion of merozoite into erythrocyte. However, the other *P. falciparum* RON proteins have yet to be characterized. Here, we determined that "PFL2505c" (hereafter referred to as *pfron3*) is the ortholog of the *tgron3* in *P. falciparum* and characterized its protein expression profile, subcellular localization, and complex formation. Protein expression analysis revealed that *Pf*RON3 was expressed primarily in late schizont stage parasites. Immunofluorescence microscopy (IFA) showed that *Pf*RON3 localizes in the apical region of *P. falciparum* merozoites. Results from immunoelectron microscopy, along with IFA, clarified that *Pf*RON3 localizes in the rhoptry body and not in the rhoptry neck. Even after erythrocyte invasion, *Pf*RON3 was still detectable at the parasite ring stage in the parasitophorous vacuole. Moreover, co-immunoprecipitation studies indicated that *Pf*RON3 interacts with *Pf*RON2 and *Pf*RON4, but not with *Pf*AMA1. These results suggest that *Pf*RON3 partakes in the novel *Pf*RON complex formation (*Pf*RON2, 3, and 4), but not in the moving junction complex (*Pf*RON2, 4, 5, and *Pf*AMA1). The novel *Pf*RON complex, as well as the moving junction complex, might play a fundamental role in erythrocyte invasion by merozoite stage parasites.

1. Introduction

Malaria is caused by the replication of protozoan parasites of the genus *Plasmodium* in circulating host erythrocytes [1]. The invasion process of merozoite stage parasite into erythrocyte requires the discharge of contents of apical secretory organelles (micronemes and rhoptries) to form an irreversible contact, called a tight junction, between the merozoite and the erythrocyte membrane. This tight junction migrates from the anterior to posterior poles of the merozoite. According to this moving junction, the host membrane invaginates the merozoites to eventually form a parasitophorous vacuole [2,3]. The moving junction is one of the most distinctive features of apicomplexan invasion into host cells, and was first observed in *Plasmodium* species [4]. Studies in apicomplexan parasite *Toxoplasma gondii* identified a total of four proteins from distinct apical secretory organelles to form a moving junction complex; micronemal protein apical membrane antigen 1 (AMA1) and three rhoptry neck (RON) proteins, RON2, RON4, and RON5 [5,6]. Recently, this RON–AMA1 complex (*Pf*RON2, *Pf*RON4, *Pf*RON5, and *Pf*AMA1) was also identified in *Plasmodium falciparum* [7–9]. Attempts to knockout the AMA1 gene locus were unsuccessful in both *Plasmodium* [10] and *T. gondii* [11]. AMA1-binding peptide R1 not only prevents RON–AMA1 complex interaction, but also blocks *P. falciparum* merozoite invasion into erythrocytes [9].

Although the cumulative evidence above strongly suggests that the conserved RON–AMA1 complex plays an essential role in merozoite invasion, it is yet to be clarified whether molecules other than RON2, RON 4, and RON 5, play roles in the formation of the moving junction complex and in the invasion process. The report on *T. gondii* rhoptry proteome identified the presence of other RON proteins, RON1 and RON3 [12]. Therefore, we were interested in

* Corresponding author. Cell-Free Science and Technology Research Center, Ehime University, Matsuyama, Ehime 790-8577, Japan. Tel.: +81 89 927 8277; fax: +81 89 927 9941.
E-mail address: tsuboi@ccr.ehime-u.ac.jp (T. Tsuboi).

1383-5769/$ – see front matter © 2011 Elsevier Ireland Ltd. All rights reserved.
doi:10.1016/j.parint.2011.01.001

identifying the ortholog of *tgron3* in *P. falciparum* and in characterizing its protein expression profile, subcellular localization, and role in the formation of the RON–AMA1 complex.

2. Materials and methods

2.1. Parasites

P. falciparum asexual stages (3D7 strain) were maintained in human erythrocytes (blood group O^+) *in vitro*, as previously described [13].

2.2. RNA isolation and cDNA synthesis

Total RNA was extracted from *P. falciparum* schizont-infected erythrocytes (purified by differential centrifugation on a 70%/40% Percoll/sorbitol gradient) using the TRizol Reagent (Invitrogen, Carlsbad, CA). Following DNase treatment, cDNA was generated with a random hexamer using the SuperScriptIII® First Strand Synthesis System (Invitrogen).

2.3. Antibodies

Recombinant *Pf*RON3 proteins were produced using the wheat germ cell-free translation system (CellFree Sciences, Matsuyama, Japan) as described previously [14–16]. Briefly, regions of the *Pf*RON3 gene encoding the deduced amino acid sequence, 927–1056 (*Pf*RON3_1) and 1686–1884 (*Pf*RON3_2), were PCR-amplified from *P. falciparum* 3D7 blood-stage cDNA and ligated into pEU-E01-GST-(TEV)-N2 (CellFree Sciences), an expression plasmid with an N-terminal glutathione S transferase (GST)-tag followed by a tobacco etch virus (TEV) protease cleavage site, designed specifically for the wheat germ cell-free protein expression. Oligonucleotide primers used in the PCR amplification were *Pf*RON3_XhoIF1 (5′-ctcgagGATATTCCATTAAAAGAAACCTATAAATT-3′) and *Pf*RON3_BamHIR1 (5′-ggatccCTAATGTGGGAACATTTCATGATTTGGTA-3′) for *Pf*RON3_1, and *Pf*RON3_XhoIF2 (5′-ctcgagGATTTTAAAGATAAATCAGATGATGATC-3′) and *Pf*RON3_BamHIR2 (5′-ggatccCTATTTTTTAGGTACATATATATTATATGGTC-3′) for *Pf*RON3_2 (XhoI and BamHI restriction sites are underlined). Both GST-*Pf*RON3_1 and GST-*Pf*RON3_2 were captured using a glutathione-Sepharose 4B column (GE Healthcare, Camarillo, CA), and eluted by on-column cleavage with 60 U of AcTEV protease (Invitrogen) after extensive washing with PBS. To generate anti-*Pf*RON3_1 and anti-*Pf*RON3_2 sera, female BALB/c mice were immunized subcutaneously with 20 μg of purified *Pf*RON3_1 or *Pf*RON3_2 emulsified with Freund's adjuvant. A Japanese white rabbit was also immunized subcutaneously with 250 μg of purified *Pf*RON3_1 or *Pf*RON3_2 emulsified with Freund's adjuvant. All immunizations were performed 3 times at 3-week intervals, and then antisera were collected 2 weeks after the third immunization. In a similar manner, mouse anti-*Pf*RAP1 (aa 1–782) antibody, mouse anti-*Pf*EXP2 (aa 25–287) antibody, mouse and rabbit anti-*Pf*AMA1 (aa 25–546) antibodies, and rabbit anti-GST antibody, were generated as control. Rabbit antisera against the *Pf*RON3_1 and *Pf*RON3_2 proteins were affinity purified using a column conjugated with recombinant *Pf*RON3_1 or *Pf*RON3_2 as ligands, respectively. Briefly, recombinant *Pf*RON3_1 or *Pf*RON3_2 was covalently linked to a HiTrap™ NHS-activated HP column (GE Healthcare) as manufacturer's recommendation. Rabbit antiserum was then applied to either the *Pf*RON3_1- or the *Pf*RON3_2-conjugated column. After an extensive washing step with 20 mM phosphate buffer (pH 7.0), antigen-specific IgGs were eluted with 0.1 M glycine–HCl (pH 2.5), and then immediately neutralized with 1 M Tris (pH 9.0). Mouse monoclonal anti-*Pf*RON4 antibody (26C64F12) [7] and anti-*Pf*RESA antibody (23/9) [17] were kind gifts from Jean F. Dubremetz (Université de Montpellier 2, France) and Robin F. Anders (La Trobe University, Australia), respectively.

2.4. SDS-PAGE and western blot analysis

P. falciparum cultured parasites were harvested after tetanolysin (List Biological Laboratories, Inc., Campbell, CA) treatment that can remove the hemoglobin without loss of parasite proteins present in the parasitophorous vacuolar space [18]. The parasite proteins were then extracted in SDS-PAGE loading buffer, incubated at 4 °C for 6 h, and subjected to electrophoresis under reducing condition on a 12.5% polyacrylamide gel (ATTO, Tokyo, Japan). Proteins were then transferred to a 0.2-μm PVDF membrane (GE Healthcare). The proteins were immunostained with antisera followed by horseradish peroxidase-conjugated secondary antibody (GE Healthcare) and visualized with Immobilon Western Chemiluminescent HRP Substrate (Millipore, Billerica, MA) on a LAS 4000 mini luminescent image analyzer (GE Healthcare). The relative molecular masses of the proteins were estimated with reference to Precision Plus Protein Standards (BioRad, Hercules, CA).

2.5. Immunoprecipitation

Immunoprecipitation was carried out as previously described [19]. Briefly, proteins were extracted from late schizont parasite pellets in PBS with 1% Triton X-100 containing Complete Proteinase Inhibitor Cocktail (Roche, Indianapolis, IN). Supernatants (50 μl) were pre-incubated at 4 °C for 1 h with 40 μl of 50% protein G-conjugated beads (GammaBind Plus Sepharose; GE Healthcare) in NETT buffer (50 mM Tris–HCl, 0.15 M NaCl, 1 mM EDTA, and 0.5% Triton X-100) supplemented with 0.5% BSA (fraction V; Sigma-Aldrich Corporation, St. Louis, MO). Aliquots of recovered supernatants were incubated either with rabbit anti-*Pf*RON3_1, anti-*Pf*AMA1, anti-*Pf*RON2, or anti-GST antibody, and then 40 μl of 50% protein G-conjugated bead suspension was added. After one-hour incubation at 4 °C, the beads were washed once with NETT–0.5% BSA, once with NETT, once with high-salt NETT (0.5 M NaCl), once with NETT, and once with low-salt NETT (0.05 M NaCl and 0.17% Triton X-100). Finally, proteins were eluted from the protein G-conjugated beads with 0.1 M glycine–HCl (pH 2.5), and then immediately neutralized with 1 M Tris pH 9.0. The supernatants were used for western blot analysis.

2.6. Indirect immunofluorescence assay

Thin smears of ring or schizont-enriched *P. falciparum*-infected erythrocytes were prepared on glass slides and stored at −80 °C. The smears were thawed, fixed with 4% formaldehyde at room temperature for 10 min, permeabilized with PBS containing 0.1% Triton X-100 at room temperature for 15 min, and blocked with PBS containing 5% non-fat milk at 37 °C for 30 min. The smears were then incubated with rabbit anti-*Pf*RON3 antibodies (1:500 dilution) and control mouse antibodies at 37 °C for 1 h, followed by incubation with both Alexa Fluor 488-conjugated goat anti-rabbit IgG and Alexa Fluor 546-conjugated goat anti-mouse IgG (Invitrogen) as secondary antibodies (1:500) at 37 °C for 30 min. Nuclei were stained with 4′,6-diamidino-2-phenylindole (2 μg/ml, DAPI) mixed with a secondary antibody solution. Slides were mounted in ProLong Gold Antifade reagent (Invitrogen) and viewed under ×63 oil-immersion lens. High-resolution image-capture and processing were performed using a confocal scanning laser microscope (LSM5 PASCAL or LSM710; Carl Zeiss MicroImaging, Thornwood, NY). Images were processed in Adobe Photoshop (Adobe Systems Inc., San José, CA).

2.7. Immunoelectron microscopy

Parasites were fixed for 15 min on ice in a mixture of 1% paraformaldehyde and 0.1% glutaraldehyde in 0.1 M phosphate buffer (pH 7.4). Fixed specimens were washed, dehydrated, and embedded in LR White resin (Polysciences, Inc., Warrington, PA) as previously

have been described [20,21]. Ultrathin sections were blocked in PBS containing 5% non-fat milk and 0.01% Tween 20 (PBS-MT) at 37 °C for 30 min. Grids were then incubated at 4 °C overnight with rabbit anti-*Pf*RON3_2 or control sera in PBS-MT (1:20). After washing with PBS containing 10% BlockAce (Yukijirushi, Sapporo, Japan) and 0.01% Tween 20 (PBS-BT), the grids were incubated at 37 °C for 1 h with goat anti-rabbit IgG conjugated to 10 nm gold particles (GE Healthcare) diluted 1:20 in PBS-MT, rinsed with PBS-BT, and fixed at room temperature for 10 min in 2.5% glutaraldehyde to stabilize the gold particles. The grids were then rinsed with distilled water, dried, and stained with uranyl acetate and lead citrate. Samples were examined with a transmission electron microscope (JEM-1230; JEOL, Tokyo, Japan).

3. Results

3.1. Primary structure analysis of the RON3 orthologs

Using *Tg*RON3 (TGME49_023920) as a query in BLAST analyses [22], we found RON3 orthologs in *P. falciparum* (*Pf*RON3; PFL2505c, PlasmoDB) [23], *P. yoelii* 17XNL strain (*Py*RON3; PY01808, PlasmoDB), *P. vivax* Sal-I strain (*Pv*RON3; PVX_101485, PlasmoDB), *P. knowlesi* H strain (*Pk*RON3; PKH_146960, PlasmoDB), *P. chabaudi* AS strain (*Pch*RON3; PCA_146710, PlasmoDB), *P. berghei* ANKA strain (*Pb*RON3; PBANKA_146490, PlasmoDB), and *Eimeria tenella* (*Et*RON3; CAO79912, Sanger Institute). The full-length *Pf*RON3 protein consists of 2215 amino acid residues, with a putative N-terminal signal peptide sequence predicted by SignalP3.0 [24] to span amino acid residues 1 – 22. Three transmembrane regions (TM) (aa 250–272, 276–298, and 551–573) were predicted by TMHMM2.0 [25], and one coiled coil region (aa 1822–1847) was predicted by SMART [26]. Alignment of the deduced amino acid sequences of all the RON3 orthologs among the genus *Plasmodium* using Clustal W [27] demonstrated that twelve Cys residues are conserved (Fig. 1), with a 42% overall sequence identity. Moreover, the N-terminal region is highly conserved among the RON3 orthologs in the genus *Plasmodium*, in *T. gondii*, and in *E. tenella* (Fig. 2).

3.2. PfRON3 is expressed in the schizont stage and existed in the ring stage

The PfRON3 protein expression profile was analyzed by stage-specific western blot analysis using tightly synchronized parasites as antigens. Both antibodies (α-*Pf*RON3_1 and _2) recognized a band slightly larger than 250 kDa corresponding to the predicted molecular mass of *Pf*RON3 in late stage parasites, 40–44 h post invasion (Fig. 3A, arrowhead). Furthermore, both antibodies also recognized a prominent 190-kDa band, 40–44 h post invasion (Fig. 3A, arrow). After erythrocyte invasion, the 190-kDa band quickly degraded to 50- and 40-kDa bands (Figs. 3A and 4H). However, a small amount of the 190-kDa band was present throughout the ring (Figs. 3A and 4H) and trophozoite stages (Fig. 3A, 24–36 h). Additionally, only the anti-*Pf*RON3_2 antibody recognized a 37-kDa band, 40–44 h post invasion that might represent one of the processed forms of the *Pf*RON3 protein (Fig. 3A). Neither anti-PfRON3_1 or -PfRON3_2 had any reactivity against antigens of uninfected erythrocytes (Supplementary Fig. S1).

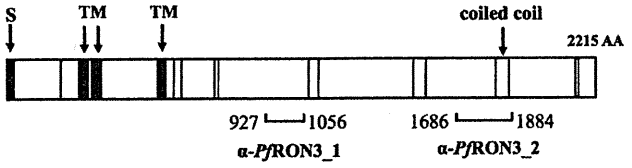

Fig. 1. Schematic representation of *Pf*RON3. The primary structure of *Pf*RON3 is depicted based on the analyses described in the Results section. S and TM indicate putative signal peptide (black) and transmembrane (blue) sequences, respectively. The yellow color box indicates a coiled coil region. Vertical red bars indicate conserved Cys residues in orthologs among the genus *Plasmodium*. The regions used to generate anti-*Pf*RON3 sera (α-*Pf*RON3_1 and α-*Pf*RON3_2) are indicated.

3.3. PfRON3 localizes in the rhoptry body of merozoites

In order to determine the sub cellular localization of *Pf*RON3, a dual label indirect immunofluorescence assay (IFA) was performed using anti-*Pf*RON3_2 antibody with anti-*Pf*RAP1 (rhoptry body marker), anti-*Pf*RON2 (rhoptry neck marker), anti-*Pf*AMA1 (microneme marker), and anti-*Pf*RESA (dense granule marker) antibodies as controls (Fig. 4). In mature schizonts, the anti-*Pf*RON3 antibody produced a punctate pattern of fluorescence in the apical end of each developing merozoite. Although some of the *Pf*RON3 signals overlapped with those of *Pf*RON2, *Pf*AMA1, or *Pf*RESA the *Pf*RON3 signals did not completely colocalize with those of the controls, whereas complete colocalization was observed between the signals of PfRON3 and *Pf*RAP1. Negative control sera were always used and these images were found to be negative (data not shown). To confirm the IFA results, the precise subcellular localization of *Pf*RON3 in the merozoite. Using anti-*Pf*RON3 antibody, gold particle signals were detected in the body portion of the rhoptries (Fig. 5).

3.4. PfRON3 is found in the parasitophorous vacuolar space after merozoite invasion into erythrocyte

To investigate *Pf*RON3 localization after the parasite invades erythrocytes, we performed IFA on ring stage parasites. *Pf*RAP1 and *Pf*EXP2 were used as parasitophorous vacuolar (PV) markers because they have been demonstrated to be present in ring stages and to associate with the PV [28–30]. We found that *Pf*RON3 colocalized with the PV markers, *Pf*RAP1 and *Pf*EXP2 in a discrete compartment surrounding the ring stage parasites (Fig. 6A). Next we performed western blot analysis using extracts of tightly synchronized ring or schizont stage parasites (Fig. 6B). *Pf*RON3 was detected in ring and schizont stage parasites together with *Pf*RAP1 and *Pf*EXP2. However *Pf*RON2 and *Pf*RON4 were detected only in schizont stage parasites (Fig. 6B) in agreement with the IFA results (Fig. 6A). Negative control sera were always used and these images were found to be negative (data not shown).

3.5. PfRON3 forms a complex with PfRON2 and PfRON4, but not with PfAMA1

To evaluate the interaction between *Pf*RON3 and the RON–AMA1 complex, we performed immunoprecipitation experiments using mature schizont-rich parasite extracts (Fig. 7). We did not detect *Pf*RON3 in the immunoprecipitate obtained using anti-*Pf*AMA1 antibody. However, PfRON3 was found in the anti-*Pf*RON2 precipitates. In the reciprocal experiment, *Pf*RON2 and *Pf*RON4 were detected in the immunoprecipitate obtained using the anti-*Pf*RON3_1 antibody; however, *Pf*AMA1 was not detected (Fig. 7). There was negligible crossreactivity between the anti-PfRON3_1 or anti-PfRON3_2 IgGs and PfRON2 and PfRON4 (Supplementary Fig. S1). These faint crossreactions were insignificant compared to the reactions with the actual target molecules.

4. Discussion

In this study, we characterized the protein expression profile and subcellular localization of *P. falciparum* RON3 as well as its complex formation with *Pf*RON2 and *Pf*RON4.

Studies of the apicomplexan parasite *T. gondii* identified various *Tg*RON proteins (RON2, RON4, RON5 [5,6], RON1, and RON3 [12]). The potential orthologs of the *Tg*RON proteins were subsequently

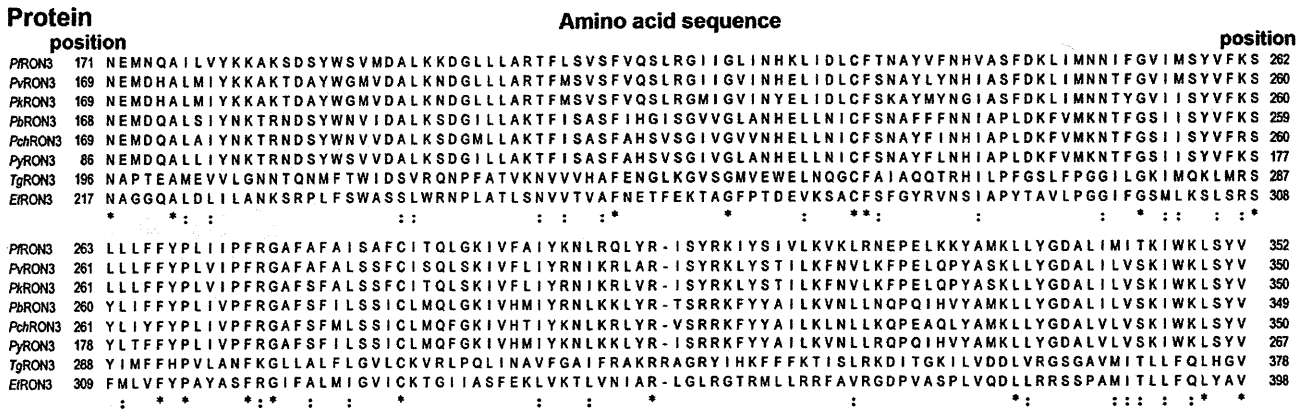

Fig. 2. Amino acid alignment of the conserved N-terminal region of RON3 orthologs. Deduced amino acid sequences of RON3 orthologs were aligned using Clustal W with manual correction. "*" indicates the conserved residues in the aligned sequences. ":" indicates conservative substitutions. Cys residues are highlighted in yellow.

identified in *P. falciparum*. Bradley et al. [12] suggested that *Pf*RON3 (PFL2505c) is an ortholog of *Tg*RON3 (TGME49_023920). However, Proellocks et al. [31] analyzed the amino acid sequence similarities of the RON orthologs identified in the genera *Plasmodium, Toxoplasma*, and some (but not all) *Apicomplexa*, and reported that, they may not be true orthologs because the collective sequence identity is below 12% [31]. In contrast, our pair-wise amino acid alignments between *T. gondii* and *P. falciparum* RON orthologs showed 11% identity between RON1 orthologs (TGME49_110010 vs. PFD0207c), 14% between RON2 orthologs(TGME49_100100 vs. PF14_0495), 12% between RON3 orthologs (TGME49_023920 vs. PFL2505c), and 10% between RON4 orthologs (TGME49_029010 vs. PF11_0168), suggesting that the amino acid identity between RON3 orthologs (*Tg*RON3 and *Pf*RON3) is comparable to that of other RON orthologs. Furthermore, multiple alignments of the deduced amino acid sequences of apicomplexan parasite RON3 orthologs showed that the N-terminal regions are conserved (Fig. 2). Based on these analyses, we conclude that *Pf*RON3 (PFL2505c) is an authentic ortholog of *Tg*RON3 (TGME49_023920).

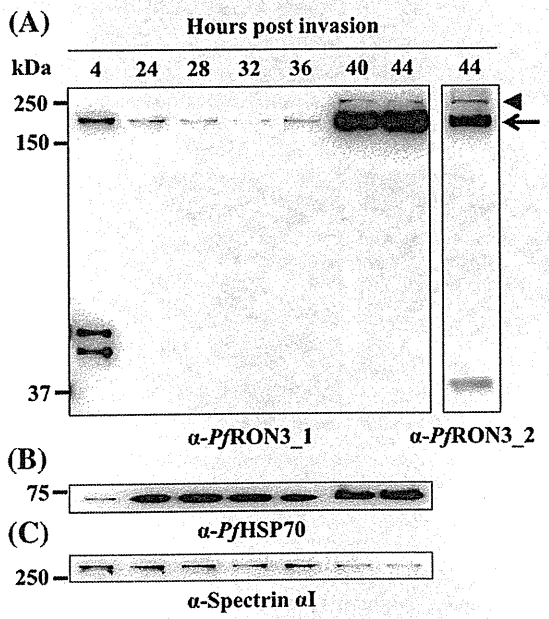

Fig. 3. Stage-specific expression profile of *Pf*RON3. Proteins from synchronized parasite cultures were harvested at each time point and separated by SDS-PAGE on a 12.5% gel under reducing condition. (A) Using either anti-*Pf*RON3_1- or anti-*Pf*RON3_2- specific antibodies, a band of approximately 260 kDa (arrowhead) was detected in late stages (40–44 h post invasion) and a 190-kDa band (arrow) was detected in both the schizont, ring, and trophozoite stage parasites. (B and C) Loading controls. To ensure that equal amounts of the stage-specific samples were loaded in each lane for western blot analysis, the membranes were probed with anti-*Pf*HSP70 monoclonal antibody (4C9) as a quantitative parasite protein marker [36], and anti-human spectrin α I rabbit antibody indicating the number of erythrocytes. The intensity of the *Pf*HSP70 bands indicated that the amount of sample loaded in each lane was comparable.

T. gondii RON3 protein was originally suggested to be localized at the rhoptry neck by immunofluorescence assay [12]. In contrast, our current immunoelectron microscopy results confirmed that *Pf*RON3 localizes in the rhoptry body rather than the rhoptry neck. Since *Pf*RON3 is in the rhoptry body, we are tempted to think that TgRON3 is also localizes in the rhoptry body rather than the rhoptry neck. Therefore we believe that the localization of *Tg*RON3 should be reconfirmed by electron microscopy using quality antibodies. In general, the biggest technical hurdle to obtaining antibodies of adequate quality for use in electron microscopy studies of this sort would be the ability to produce correctly folded recombinant proteins in sufficient quantity and purity [31]. The immunoelectron microscopy results we obtained clearly demonstrate that high quality antibodies can be successfully produced using quality proteins synthesized in the wheat germ cell-free protein production system. We have already [14–16] demonstrated that the wheat germ cell-free protein production system enables the expression of quality recombinant proteins without codon optimization.

In our stage-specific western blot and immunofluorescence microscopy analyses for the *Pf*RON3 expression profile, we detected *Pf*RON3 not only in the merozoite rhoptry body but also in the PV of ring stage parasites (Fig. 6). Previous studies showed that well-characterized rhoptry body proteins (*Pf*RhopH complex, *Pf*RAP complex, and *Pf*RAMA) are discharged into the PV [32–34]. Therefore, the secretory pathway of *Pf*RON3 into the PV might be similar to that of these rhoptry body proteins. Additionally, since the 260-kDa band, corresponding to full-length *Pf*RON3, is only visible at the schizont stage (40–44 h post invasion) (Fig. 3A), the processed 190-kDa fragment may contain the functional domains throughout the parasite's asexual erythrocytic cycle.

Finally, our immunoprecipitation studies demonstrated that *Pf*RON2, *Pf*RON3, and *Pf*RON4, are able to interact and form a novel complex *in vitro*, even in the absence of *Pf*AMA1, indicating that the formation of this novel RON complex is independent of *Pf*AMA1. These results are in agreement with the previously published results showing that *Pf*RON2 and *Pf*RON4 are able to interact and form a complex independently, in the absence of *Pf*AMA1 and in the parasite; most AMA1 is not associated with complexes that contain *Pf*RON2 and *Pf*RON4 [35]. However, in this study we were unable to confirme the